
MODELING OF 2D SELF-DRIFTING FLAME-BALLS IN HELE-SHAW CELLS

A PREPRINT

Jorge Yanez*

Institute for Thermal Energy Technology and Safety
Karlsruhe Institute of Technology
Hermann-von-Helmholtz-Platz, 1
Karlsruhe, Germany.
jorge.yanez@kit.edu

Leonid Kagan

School of Mathematical Sciences,
Tel Aviv University
Tel Aviv, Israel.
kaganleo@tauex.tau.ac.il

Gregory Sivashinsky

School of Mathematical Sciences,
Tel Aviv University
Tel Aviv, Israel.
grishas@tauex.tau.ac.il

Mike Kuznetsov

Institute for Thermal Energy Technology and Safety
Karlsruhe Institute of Technology
Hermann-von-Helmholtz-Platz, 1
Karlsruhe, Germany.
mike.kuznetsov@kit.edu

ABSTRACT

The disintegration of near limit flames propagating through the gap of Hele-Shaw cells has recently become a subject of active research. In this paper, the flamelets resulting from the disintegration of the continuous front are reinterpreted in terms of the Zeldovich flame-balls stabilized by volumetric heat losses. A complicated free-boundary problem for 2D self-drifting near circular flamelets is reduced to a 1D model. The 1D formulation is then utilized to obtain the locus of the flamelet velocity, radius, heat losses and Lewis numbers at which the self-drifting flamelet exists.

Keywords 2D Flame-balls · Flame disintegration · Combustion theory

1 Introduction

In their book *The Mathematical Theory of Combustion*, Zeldovich et al. [1] analysed theoretically the possibility of diffusively burning 3D spherical flame-balls. The occurrence of such configurations in 2D was specifically discarded. It was concluded that spherical flame-balls surrounded by motionless fluid are unstable. The authors then conjectured that flame-balls might be stabilized by radiative or convective heat losses. In the latter case, a motion would develop that in turn would modify the topology of the flame-ball which would assume the shape of a stocking-cap with a seemingly extinguished rear side.

Flame-balls were originally predicted in Zeldovich's book *Theory of Combustion and Detonation*, Acad. Sci. USSR, 1944, translated to English in [2]. Some years later, flame-balls were observed for the first time in microgravity, by Ronney and his collaborators, both in drop-tower experiments [3] and in the spacecraft [4]. Flame-balls were thereupon studied by Buckmaster et al. in a now classical series of theoretical papers [5, 6, 9, 8, 7] successfully refining the premises employed. Originally, a stationary spherical flame subjected to internal volumetric heat losses was considered [5]. The quenching limits were obtained as well as a set of radii for which the resulting spherical structure is stable and could thus be observed. The original formulation [5] was extended in [6] to incorporate heat losses in the unreacted mixture, refining the stability domain. The stability issue was later comprehensively explored numerically by Bockhorn et al. [10, 11, 12]. The assumption of no-advection in [5, 6] was relaxed in [8], where the effect of the Peclet number was also assessed. The premise of volumetric heat losses was extended to incorporate also the effect of conductive heat

*Corresponding author

losses to a neighbouring wall [7]. The theory developed in [5, 6] was applied to hydrogen-air mixtures [9] subjected to radiative heat losses. The equivalence ratios ensuring the existence of flame-balls were obtained. Finally, Grcar [13] showed that stable cell-like flamelets subjected to convective (rather than radiative) heat losses are also possible.

An unconventional disintegration of near-limit low Peclet number flames evolving in the narrow gap of Hele-Shaw cells has recently become the subject of energetic experimental and numerical research [14, 15, 16]. Physically the issue is clearly related to the problem of unconfined 3D flame-balls [5, 6, 9, 8, 7].

Isolated flamelets propagating in a narrow gap between two parallel plates were photographed by Veiga et al. [14] for Peclet numbers below 15. Among the regimes reported in [14, 15] we focus in the present paper on the regimes shown in the Figure 1, in which flamelets propagate in a quasi-stationary regime.

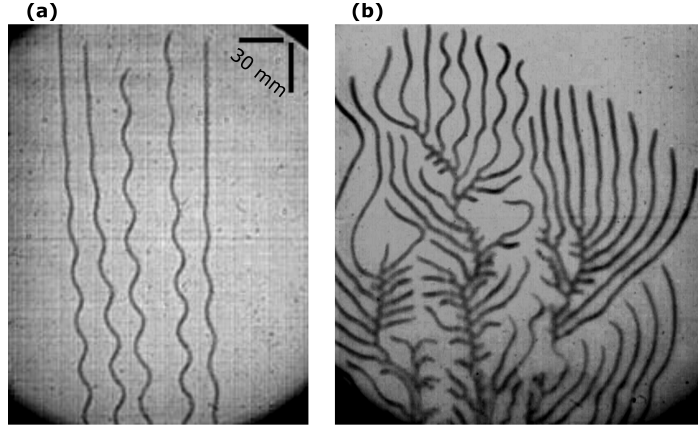


Figure 1: Monocellular hydrogen-air flamelets propagating through narrow gaps: (a) one-headed finger, (b) one-headed branching. Taken from Yanez et al. [15].

The shallow geometry of the Hele-Shaw cell suggests a 2D approach to the phenomenon. Kagan and Sivashinsky [17] studied the effect of volumetric heat losses on breaking up the flame in 2D. They assessed the changes of the front topology caused by different levels of heat losses. Some of the patterns observed are shown in Figures 2-3. A 2D geometry was also utilized by Martinez-Ruiz et al. [16] to reproduce numerically the flamelets, obtaining the stocking-cap flame shapes predicted by Zeldovich et al. [1].

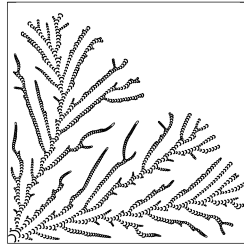


Figure 2: Successive monocellular flamelets under conductive heat losses. Simulation of the reaction-diffusion system [17] at $Q = q(T - \sigma)$ for $N = 10$, $\sigma = 0.2$, $Le = 0.25$, $q = 0.14$. The picture shows the reaction rate Ω distribution at several consecutive equidistant instants of time under initial conditions,

$$T(x, y, 0) = (1 - \sigma) \exp[-(x^2 + y^2)/l^2] + \sigma, C(x, y, 0) = 1, l = 0.25, \text{ and adiabatic boundary conditions;} \\ 0 < x, y < 240, 0 < t < 740.$$

There is an important distinction between the 3D and effectively the 2D situation typical of large aspect ratio Hele-Shaw cells. The 3D case allows for stationary spherical flame-balls which may bifurcate into a self-drifting mode [18, 19, 20, 21]. In the 2D case, the non-drifting circular flame-balls are ruled out since they cannot meet boundary conditions at infinity (due to the logarithmic tail of the associated concentration profiles [16]). So, in narrow gaps

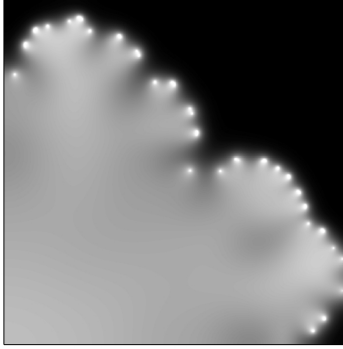


Figure 3: Distribution of the deficient reactant concentration C in 2D monocellular flamelets at $t = 740$. The lighter regions correspond to lower concentration. For conditions see the legend for Fig. 2

2D self-drifting flame-balls should emerge not as a bifurcation but rather as the only way for the 2D flame-balls to exist. Note that Ref. [18] was utilized in [22] to derive velocity, size and temperature of the flamelets appearing in the experiments of [14] on Hele-Shaw cells.

Taking into account the considerations of the previous paragraphs, the objective of this paper is to ascertain the conditions that allow for self-drifting 2D flamelets subjected to conductive heat losses. Specifically, we will derive approximate expressions for the velocity, size and temperature of the flamelet. Conceptually, our study is a link between the flame topology suggested by Zeldovich et al. [1] and the experimental findings of [14, 15]. The present paper offers a simple 1D model for 2D self-drifting flame-balls.

2 Model

2.1 General

Let us consider the problem of a stationary near-circular flamelet of diameter $2R$ propagating in an infinite Hele-Shaw cell at a constant speed V . The reaction occurs within a thin interface preceded and followed by tails where diffusion of heat and reactants take place. The flamelet propagates from right to left (Figure 4), so that in the reference frame attached to the flamelet the flow velocity is directed from left to right.

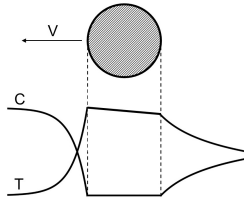


Figure 4: Up: Top sketch view of the flamelet in a plane parallel both to the paper and to the plates of the Hele-Shaw cell. Down: Profiles of temperature, T , and concentration, C , through the center of the flame-ball.

2.2 Formulation

2.2.1 General considerations

The mathematical model employed is based on the constant-density reaction-diffusion formulation [17, 18, 22, 23]. The flamelet velocity V (Figure 4) is regarded as an eigenvalue of the problem. The system of pertinent appropriately

nondimensionalized equations read,

$$\mathbf{V} \cdot \nabla T = \nabla^2 T + (1 - \sigma)\Omega - Q, \quad (1)$$

$$\mathbf{V} \cdot \nabla C = \frac{1}{Le} \nabla^2 C - \Omega, \quad (2)$$

where \mathbf{V} is the flow-field in units of U_b , the speed of a planar adiabatic flame; T the temperature in units of T_b , the adiabatic temperature of combustion products; C the concentration of the deficient reactant in units of C_0 , its value in the fresh mixture; $\nabla = (\partial/\partial x, \partial/\partial y)$ the gradient where x, y are spatial coordinates in units of $l_{th} = D_{th}/U_b$, the thermal width of the flame; $D_{th} =$ thermal diffusivity of the mixture; $\sigma = T_0/T_b$, where T_0 is the temperature sustained at the walls of the Hele-Shaw cell. Additionally, $Q = q(T - \sigma)$ represents the scaled volumetric heat loss; q stays for the scaled heat loss intensity specified as $(\pi l_{th}/d)^2$, where d the width of the Hele-Shaw gap; $Le = D_{th}/D_{mol}$ is the Lewis number, where D_{mol} is the molecular diffusivity of the deficient reactant; $N = T_a/T_b$ is the scaled activation energy, where $T_a =$ activation temperature; $\Omega(C, T) = \frac{1}{2}(1 - \sigma)^2 Le^{-1} N^2 C \exp[N(1 - T^{-1})]$ is the appropriately normalized reaction rate to ensure that at large N the scaled speed of the planar adiabatic flame is close to unity. In polar coordinates the operators ∇, ∇^2 read,

$$\nabla \square = \cos \theta \frac{\partial \square}{\partial r} - \frac{\sin \theta}{r} \frac{\partial \square}{\partial \theta}, \quad (3)$$

$$\nabla^2 \square = \frac{\partial^2 \square}{\partial r^2} + \frac{1}{r} \frac{\partial \square}{\partial r} + \frac{1}{r^2} \frac{\partial^2 \square}{\partial \theta^2}, \quad (4)$$

where \square stays for T or C . The thermo-diffusive model of [23] assumes a large activation energy, N . This simplification allows to treat the reaction zone as an infinitely thin interface, characterized by the locus $r = R(\theta)$. As a result, the reaction rate adopts a simple expression,

$$\Omega = \sqrt{1 + \frac{1}{R^2} \left(\frac{\partial R}{\partial \theta} \right)^2} \exp \left(\frac{N}{2} \left(1 - \frac{1}{T_f} \right) \right) \delta(r - R(\theta)), \quad (5)$$

where δ is the Dirac delta function, and $T_f = T(r = R(\theta))$ is the temperature at the flame-ball interface.

In Eq. (5) $R^{-2}(\partial R/\partial \theta)^2 = (\partial R/\partial s)^2$ where $ds = R d\theta$ is the arc-length element of the flame interface, $r = R(\theta)$. Reduction of the reaction-diffusion system (1)-(2) to a free-boundary problem, valid for $N \gg 1$, is a widely used procedure in premixed flame theory (see e.g. [23]).

2.2.2 Boundary conditions

For the problem considered, the boundary conditions at $r \rightarrow \infty$ read,

$$C \rightarrow 1, \quad T \rightarrow \sigma. \quad (6)$$

For $r \leq R(\theta)$,

$$C \equiv 0. \quad (7)$$

At the flame interface, $r = R(\theta)$, $T = T_f(\theta)$, $C = 0$,

$$\left[\frac{\partial T}{\partial n} \right]_-^+ = \frac{1 - \sigma}{Le} \left[\frac{\partial C}{\partial n} \right]_-^+, \quad (8)$$

$$\frac{1}{Le} \left[\frac{\partial C}{\partial n} \right]_-^+ = - \exp \left(\frac{N}{2} \left(1 - \frac{1}{T_f} \right) \right), \quad (9)$$

where the normal derivative in polar coordinates reads,

$$\frac{\partial \square}{\partial n} = \frac{\frac{\partial \square}{\partial r} - \frac{1}{R^2} \frac{\partial R}{\partial \theta} \frac{\partial \square}{\partial \theta}}{\sqrt{1 + \frac{1}{R^2} \left(\frac{\partial R}{\partial \theta} \right)^2}}. \quad (10)$$

Note that $T_f(\theta)$ is an unknown function to be determined.

2.3 Solutions

In the formulation adopted outside the flame front interface, $r = R(\theta)$, Eqs. (1)-(2) may be presented in the following unified form,

$$\frac{\partial^2 \square}{\partial r^2} + \frac{1}{r} \frac{\partial \square}{\partial r} + \frac{1}{r^2} \frac{\partial^2 \square}{\partial \theta^2} = 2k \left[\cos \theta \frac{\partial \square}{\partial r} - \frac{\sin \theta}{r} \frac{\partial \square}{\partial \theta} \right] - q(T - \sigma). \quad (11)$$

Here $2k = V$ for T -equation and $q = 0$, $2k = VLe$ for C -equation. Solutions of equation (11) are known [24, 25]. Outside the flame-ball, at $q = 0$,

$$\square = \sum_m A_m \exp(kr \cos \theta) \cos m\theta K_m(kr) + F, \quad (12)$$

while inside the flame-ball, at $q = 0$,

$$\square = \sum_m B_m \exp(kr \cos \theta) \cos m\theta I_m(kr) + G, \quad (13)$$

where K_m, I_m are the modified Bessel functions of first and second kind and A_m, B_m, F, G are parameters to be determined by the boundary conditions. Particular solutions pertinent to $q > 0$ will be treated later.

2.4 Simplification and rescaling

For further analysis it is convenient to make the following change of variables and parameters,

$$T = \sigma + (1 - \sigma)\Theta, \quad (14)$$

$$Q = (1 - \sigma)q\Theta, \quad (15)$$

$$\beta = (1 - \sigma)N. \quad (16)$$

At $(1 - \sigma) \ll 1$ and $\beta = N(1 - \sigma) \gg 1$,

$$\frac{1}{2}N\left(1 - \frac{1}{T_f}\right) \simeq \frac{1}{2}\beta(\Theta_f - 1), \quad (17)$$

where Θ, q are the re-scaled temperature and heat losses and β is the Zeldovich number. So, equations (1)-(2) become,

$$V \left(\cos \theta \frac{\partial \Theta}{\partial r} - \frac{\sin \theta}{r} \frac{\partial \Theta}{\partial \theta} \right) = \nabla^2 \Theta + \Omega - q\Theta, \quad (18)$$

$$V \left(\cos \theta \frac{\partial C}{\partial r} - \frac{\sin \theta}{r} \frac{\partial C}{\partial \theta} \right) = \frac{1}{Le} \nabla^2 C - \Omega, \quad (19)$$

$$\Omega = \sqrt{1 + \frac{1}{R^2} \left(\frac{\partial R}{\partial \theta} \right)^2} \exp \left\{ \frac{1}{2} \beta (\Theta_f - 1) \right\} \delta(r - R(\theta)). \quad (20)$$

2.5 Near-equidiffusive (NED) approximation

We continue the analysis adopting the NED approximation [23]. Let us combine (18) and (19) to obtain,

$$V \left(\cos \theta \frac{\partial (\Theta + C - 1)}{\partial r} - \frac{\sin \theta}{r} \frac{\partial (\Theta + C - 1)}{\partial \theta} \right) = \nabla^2 \left[\Theta + \frac{1}{Le} C - 1 \right] - q\Theta. \quad (21)$$

In the NED limit, Lewis number is represented as $Le = 1 - \alpha/\beta$ where β is regarded as a large parameter and α is a parameter of order one. In this approximation it is convenient to introduce the *scaled excess enthalpy*,

$$S = (\Theta + C - 1)\beta. \quad (22)$$

At $\beta \gg 1$ we set,

$$\frac{1}{Le} = 1 + \frac{\alpha}{\beta}, \quad (23)$$

$$\Theta = \Theta^{(0)} + \frac{1}{\beta}\Theta^{(1)} + \dots, \quad (24)$$

$$C = C^{(0)} + \frac{1}{\beta}C^{(1)} + \dots, \quad (25)$$

$$q = \frac{1}{\beta}\nu, \quad (26)$$

where superscripts in (24)-(25) mark the order of the $1/\beta$ expansions; ν is the heat loss parameter of order one. Accounting for equations (21)-(26) one obtains,

$$V \left(\cos \theta \frac{\partial S}{\partial r} - \frac{\sin \theta}{r} \frac{\partial S}{\partial \theta} \right) = \nabla^2 [S + \alpha C^{(0)}] - \nu \Theta^{(0)}, \quad (27)$$

$$V \left(\cos \theta \frac{\partial \Theta^{(0)}}{\partial r} - \frac{\sin \theta}{r} \frac{\partial \Theta^{(0)}}{\partial \theta} \right) = \nabla^2 \Theta^{(0)} + \Omega, \quad (28)$$

$$V \left(\cos \theta \frac{\partial C^{(0)}}{\partial r} - \frac{\sin \theta}{r} \frac{\partial C^{(0)}}{\partial \theta} \right) = \nabla^2 C^{(0)} - \Omega. \quad (29)$$

Considering the boundary conditions, equations (28) and (29) readily yield,

$$\Theta^{(0)} + C^{(0)} = 1. \quad (30)$$

This last expression allows rewriting (27) in terms of S and $\Theta^{(0)}$. The system of equations (27)-(29) thus becomes,

$$V \left(\cos \theta \frac{\partial S}{\partial r} - \frac{\sin \theta}{r} \frac{\partial S}{\partial \theta} \right) = \nabla^2 [S - \alpha \Theta^{(0)}] - \nu \Theta^{(0)}, \quad (31)$$

$$V \left(\cos \theta \frac{\partial \Theta^{(0)}}{\partial r} - \frac{\sin \theta}{r} \frac{\partial \Theta^{(0)}}{\partial \theta} \right) = \nabla^2 \Theta^{(0)} + \Omega. \quad (32)$$

At $r = R(\theta)$ we have,

$$[S]_-^+ = 0, \quad \Theta^{(0)} = 1, \quad (33)$$

$$\left[\frac{\partial S}{\partial n} \right]_-^+ = \alpha \left[\frac{\partial \Theta^{(0)}}{\partial n} \right]_-^+, \quad (34)$$

$$\left[\frac{\partial \Theta^{(0)}}{\partial n} \right]_-^+ = -\sqrt{1 + \frac{1}{R^2} \left(\frac{\partial R}{\partial \theta} \right)^2} \exp \left(\frac{1}{2} S \right). \quad (35)$$

The problem is thus reformulated in terms of S and $\Theta^{(0)}$ and parameters α, ν . It does not involve the Zeldovich number β . Inside the flame-ball, $r < R(\theta)$, one has $\Theta^{(0)} \equiv 1$.

2.6 Reduction to 1D model

As it stands the formulated 2D free-boundary problem (31)-(35) is too difficult for a straightforward analytical treatment. We therefore propose its low-mode collocation-like reduction to a 1D model that we believe will keep enough contact with the original 2D formulation.

In the 1D approach one deals with a single spatial variable z which runs from $z = -\infty$ to $z = \infty$ and in which the interior of the flame-ball covers the interval $-R < z < R$. In the expansions (12)-(13) we will keep only the leading terms corresponding to $m = 0$. Moreover, we will set $\theta = 0$ for $z > 0$ and $\theta = \pi$ for $z < 0$.

Conditions on the flame-ball interface $z = \pm R$ then become $[\Theta^{(0)}]_-^+ = [\Theta^{(1)}]_-^+ = [S]_-^+ = 0$ -continuity and the slope jumps,

$$\left[\frac{d\Theta^{(0)}}{dz} \right]_-^+ + \exp \left(\frac{1}{2} S \right) = 0, \quad (36)$$

$$\left[\frac{dS}{dz} \right]_-^+ = \alpha \left[\frac{d\Theta^{(0)}}{dz} \right]_-^+. \quad (37)$$

Moreover, we have the conditions at infinity, $\Theta(z = \pm\infty) = 0$, $S(z = \pm\infty) = 0$, $C(z = \pm\infty) = 1$ and full consumption of the deficient reactant in the interior of the flame-ball, $C(-R < z < R) = 0$.

In the simplification employed one neglects deviation of the flame-ball shape from ideal circle. This deviation however is deemed to be small. In the construction of an approximate solution, rather than working with Eqs. (31)-(35), we truncate the series involving an infinite number of terms, as in Eqs. (12)-(13), to deal with sums involving only a finite number of terms.

For a given V the problem is over-determined due to the boundary condition $\Theta^{(0)} = 1$ or $C^{(0)}$ at the front (see Eq. (30)). It is solvable only for the specific relation between V , α and ν .

2.7 Inner heat loss model

It is instructive first to consider the mathematically simplest situation accounting for the heat loss only within the flame-ball interior, setting $q = 0$ for $|z| > R$. As a result one ends up with the following system. For $\Theta^{(0)}$,

$$\Theta^{(0)}(z < -R) = \exp\left(\frac{1}{2}V(z+R)\right) \frac{K_0\left(-\frac{1}{2}Vz\right)}{K_0\left(\frac{1}{2}VR\right)}, \quad (38)$$

$$\Theta^{(0)}(z > R) = \exp\left(\frac{1}{2}V(z-R)\right) \frac{K_0\left(\frac{1}{2}Vz\right)}{K_0\left(\frac{1}{2}VR\right)}, \quad (39)$$

$$\Theta^{(0)}(-R < z < R) = 1. \quad (40)$$

For $\Theta^{(1)}$ a similar procedure can be undertaken, considering the external solution (12) applied to the equation for S , (31). Considering the definition of the *excess enthalpy* (22), zero order expansion (30) and the boundary conditions (7) one readily obtains,

$$\Theta^{(1)}(z > R) = S_+ \Theta^{(0)}(z > R), \quad (41)$$

$$\Theta^{(1)}(z < -R) = S_- \Theta^{(0)}(z < -R), \quad (42)$$

$$\Theta^{(1)}(-R < z < R) = S(-R < z < R), \quad (43)$$

where $S_+ = \Theta^{(1)}(R)$ and $S_- = \Theta^{(1)}(-R)$.

For S , as follows from its definition (22), and the zero order approximation (30),

$$S(z > R) = \Theta^{(1)}(z > R) + C^{(1)}(z > R), \quad (44)$$

$$S(z < -R) = \Theta^{(1)}(z < -R) + C^{(1)}(z < -R). \quad (45)$$

Inside the flame-ball, a simplified expression for S can be constructed from the solution (13) augmented with the heat loss term,

$$S(-R < z < R) = A + B \exp\left(\frac{1}{2}Vz\right) I_0\left(\frac{1}{2}V|z|\right) - \frac{\nu}{V}z, \quad (46)$$

where the constants,

$$A = \frac{1}{2}(S_+ + S_-) - \frac{1}{2}BI_0\left(\frac{1}{2}VR\right) \left(\exp\left(\frac{1}{2}VR\right) + \exp\left(-\frac{1}{2}VR\right)\right), \quad (47)$$

$$B = \frac{2\nu R + V(S_+ - S_-)}{VI_0\left(\frac{1}{2}VR\right) \left(\exp\left(\frac{1}{2}VR\right) - \exp\left(-\frac{1}{2}VR\right)\right)}. \quad (48)$$

arise from the continuity conditions at $\pm R$. Relations for $C^{(1)}$, are based on the equations,

$$C(z > R) = 1 - \exp\left[\frac{1}{2}VLe(z-R)\right] \frac{K_0\left(\frac{1}{2}VLez\right)}{K_0\left(\frac{1}{2}VLeR\right)}, \quad (49)$$

$$C(z < -R) = 1 - \exp\left[\frac{1}{2}VLe(z+R)\right] \frac{K_0\left(-\frac{1}{2}VLez\right)}{K_0\left(\frac{1}{2}VLeR\right)}. \quad (50)$$

Here equations (49)-(50) are similar to (38)-(39) where V is replaced by VLe and boundary conditions $\Theta^{(0)}(\pm R) = 1$ are replaced by $C(\pm R) = 0$. Considering $1/\beta$ expansions and Eq. (23), one obtains,

$$C^{(1)}(z > R) = -\frac{1}{2}V\alpha \left[\frac{K_1(\frac{1}{2}Vz)}{K_0(\frac{1}{2}Vz)}z - \frac{K_1(\frac{1}{2}VR)}{K_0(\frac{1}{2}VRz)}R - (z - R) \right] \Theta^{(0)}(z > R), \quad (51)$$

$$C^{(1)}(z < -R) = \frac{1}{2}V\alpha \left[\frac{K_1(-\frac{1}{2}Vz)}{K_0(-\frac{1}{2}Vz)}z + \frac{K_1(\frac{1}{2}VR)}{K_0(\frac{1}{2}VRz)}R + (z + R) \right] \Theta^{(0)}(z < -R), \quad (52)$$

$$C^{(1)}(-R < z < R) = 0. \quad (53)$$

Substituting the above relations into (36)-(37) one ends up with a system determining S_+ , S_- , V and R .

2.8 Global heat losses

Let us consider the equation (18) for Θ at $r > R(\theta)$,

$$2k \left(\cos \theta \frac{\partial \Theta}{\partial r} - \frac{\sin \theta}{r} \frac{\partial \Theta}{\partial \theta} \right) = \nabla^2 \Theta - q\Theta. \quad (54)$$

For $m = 0$ the solutions of (54) may be sought (see (12)) as,

$$\Theta = \exp(kr \cos \theta) f(r). \quad (55)$$

Substituting this into (54), one obtains,

$$\Theta = H \exp(kr \cos \theta) K_0 \left(\sqrt{k^2 + qr} \right), \quad (56)$$

H being a constant. This allows us to draw an important conclusion: the only effect of the heat loss term $q\Theta$ outside the flame-ball is the shrinking of the K_0 -function, compared to the $q = 0$ case.

For the 1D modeling adopted in this study Eq. (56) implies,

$$\Theta(z > R) = \left(1 + \frac{1}{\beta} S_+ \right) \exp[k(z - R)] \frac{K_0 \left(\sqrt{k^2 + qz} \right)}{K_0 \left(\sqrt{k^2 + qR} \right)}, \quad (57)$$

$$\Theta(z < -R) = \left(1 + \frac{1}{\beta} S_- \right) \exp[k(z + R)] \frac{K_0 \left(-\sqrt{k^2 + qz} \right)}{K_0 \left(\sqrt{k^2 + qR} \right)}. \quad (58)$$

3 Locus of V , R , ν

3.1 System of equations

Four equations (36)-(37) determine four unknowns of the problem, S_+ , S_- , V , R . But since $\partial \Theta^{(0)}(-R^+)/\partial z = \partial \Theta^{(0)}(R^-)/\partial z = 0$, equations (36) readily imply that,

$$S_+ = 2 \ln \left[-\frac{\partial \Theta^{(0)}(R^+)}{\partial z} \right], \quad (59)$$

$$S_- = 2 \ln \left[\frac{\partial \Theta^{(0)}(-R^-)}{\partial z} \right]. \quad (60)$$

Therefore, the number of equations and unknowns are reduced to two. Inside the flamelet, equation (46) provides S , so that finally,

$$\frac{dS(R^+)}{dz} - \left\{ \frac{1}{2}BV \exp\left(\frac{1}{2}VR\right) \left[I_0\left(\frac{1}{2}VR\right) + I_1\left(\frac{1}{2}VR\right) \right] - \frac{\nu}{V} \right\} = \alpha \frac{d\Theta^{(0)}(R^+)}{dz}, \quad (61)$$

$$\frac{dS(-R^-)}{dz} - \left\{ \frac{1}{2}BV \exp\left(-\frac{1}{2}VR\right) \left[I_0\left(\frac{1}{2}VR\right) - I_1\left(\frac{1}{2}VR\right) \right] - \frac{\nu}{V} \right\} = \alpha \frac{d\Theta^{(0)}(-R^-)}{dz}. \quad (62)$$

To close this problem, we need to present expressions for $d\Theta^{(0)}(-R^-)/dz$, $d\Theta^{(0)}(R^+)/dz$, $dS(-R^-)/dz$ and $dS(R^+)/dz$.

The derivatives of $\Theta^{(0)}$ can be obtained directly from equations (38)-(39). Expressions for derivatives of S are provided by Eqs. (44)-(45) and (51)-(52). Here the formula for $\Theta^{(1)}$ depends on whether one considers the inner or global heat losses. For inner heat losses, $\Theta^{(1)}$ is specified by Eqs. (51)-(52), whilst for global heat losses Eqs. (57) and (58) should be employed. In the latter case,

$$\frac{dS(R^+)}{dz} = S_+ \frac{d\Theta^{(0)}(R^+)}{dz} - \Sigma, \quad (63)$$

$$\frac{dS(-R^-)}{dz} = S_- \frac{d\Theta^{(0)}(-R^-)}{dz} + \Sigma, \quad (64)$$

where

$$\Sigma = \left(\frac{\nu}{V} + \frac{V\alpha}{2} \right) \left\{ \frac{VR}{4} \left[\frac{2K_1^2 \left(\frac{1}{2}VR\right) - K_0^2 \left(\frac{1}{2}VR\right) - K_0 \left(\frac{1}{2}VR\right) K_2 \left(\frac{1}{2}VR\right)}{K_0^2 \left(\frac{1}{2}VR\right)} \right] + \frac{K_1 \left(\frac{1}{2}VR\right)}{K_0 \left(\frac{1}{2}VR\right)} \right\} + \frac{V\alpha}{2}, \quad (65)$$

and

$$\frac{d\Theta^{(0)}(R^+)}{dz} = \frac{V}{2} \left[1 - \frac{K_1 \left(\frac{1}{2}VR\right)}{K_0 \left(\frac{1}{2}VR\right)} \right], \quad (66)$$

$$\frac{d\Theta^{(0)}(-R^-)}{dz} = \frac{V}{2} \left[1 + \frac{K_1 \left(\frac{1}{2}VR\right)}{K_0 \left(\frac{1}{2}VR\right)} \right]. \quad (67)$$

For the inner heat loss model ν in Eq. (65) should be set at zero.

3.2 Numerical procedure

In spite of its apparent complexity, for a fixed α , (61)-(62) is a system of two equations with two unknowns, R , V , and a parameter ν . For brevity let us denote the system of equations by \mathbf{f} and the variables by \mathbf{y} .

The loci of solutions of complex non-linear systems may contain bifurcation or turning points that make naive direct solutions by direct successive application of root-finding algorithms ineffective. Therefore, the so-called *continuation principle* [26] has been utilized to obtain the *-parametric-* solution.

The procedure regards the solution as a function of a certain arc-length, s , which is constructed with the unknowns \mathbf{y} and the parameter ν . A single *-initial-* solution of the equations is then obtained utilising any root-finding algorithm, in our case Newton-Raphson method which is readily available in Sympy [27]. Considering the Jacobian of the equations, a tangent is traced which allows finding a nearby solution by a predictor-corrector methodology. Since the system,

$$0 = d\mathbf{f} = \mathbf{f}_y d\mathbf{y} + \mathbf{f}_\nu d\nu, \quad (68)$$

is undetermined, it must be complemented with a so-called *parametrization*. Among the different available formulations [26], we choose it to be

$$\sum_i dy_i^2 + d\nu^2 - ds^2 = 0, \quad (69)$$

where ds is an imposed arc-length increment, small enough to obtain the necessary accuracy and fulfill stability requirements.

The so called *direct method* we are utilizing requires the calculation of the extended Jacobian $[\mathbf{f}_y, \mathbf{f}_\nu]$. Such derivation is feasible for our system, since it has only two equations, two unknowns and one parameter. Nevertheless, the algebra involved is very extensive requiring the utilization of a symbolic algebra package, in our case, Sympy [27].

We refer the reader to the monograph of Seydel[26] for further technical details.

3.3 Results. Locus V - R - ν - α

The numerical procedure outlined in section 3.2 applied to equations (61)-(62) readily yields the dependencies shown in Figures 5, 6, 7, when the heat losses outside the flame-ball are suppressed. For global heat losses the pertinent diagrams are displayed in Figures 8, 9, 10.

One can draw several conclusions from the the results obtained.

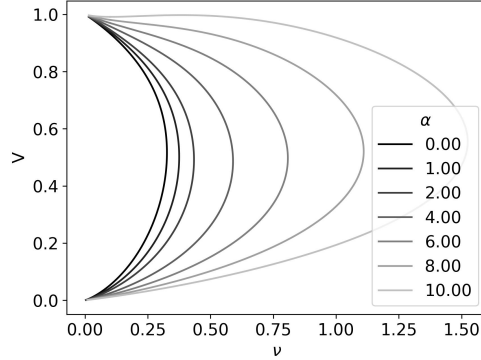


Figure 5: Locus of the velocities, V , as a function of the heat losses, ν , for different Lewis number parameters, α . Inner heat losses.

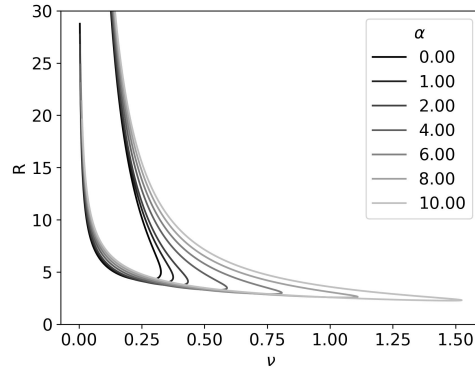


Figure 6: Locus of the flamelet radii, R , as a function of the heat losses, ν , for different Lewis number parameters, α . Inner heat losses.

1. Parameter α strongly affects $V(\nu)$, $R(\nu)$ dependencies. The heat loss intensity at the quenching (turning) point (ν_q) increases with the decrease of the Lewis number, $Le = 1 - \alpha/\beta$.
2. Accounting for the heat loss outside the flame-ball ($|z| > R$) leads to a reduction of ν_q .
3. At $\nu < \nu_q$ the multiplicity of $V(\nu)$, $R(\nu)$ dependencies is observed where only the regime with decreasing $V(\nu)$ is likely to be dynamically feasible. This would be in line both with numerical simulations [16] as well as recent experimental studies [28].

A similar non-uniqueness is known to occur in planar ($R = \infty$) non-adiabatic flames allowing for a comprehensive theoretical analysis which leads to the following α -independent relation between V and ν [29],

$$V^2 \ln \left(\frac{1}{V} \right) = \nu. \quad (70)$$

4. A significant drop of temperature at the rear side ($z = R$) of the self-drifting flame-ball might explain the stoking-cap shape of the advancing flamelet. The later is often perceived as a local extinction (opening) of the front.

3.4 Profiles across the flame-ball

Once the solutions for $V(\nu)$, $R(\nu)$, for a certain α are available, we can plot $\Theta^{(0)}$, Θ and S vs. z .

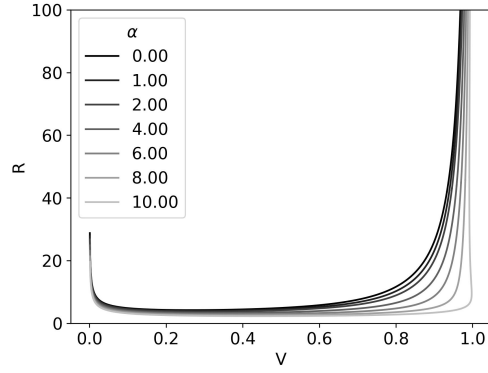


Figure 7: Locus of the flamelet radii, R , as a function of the velocities, V , for different Lewis number parameters, α . Inner heat losses.

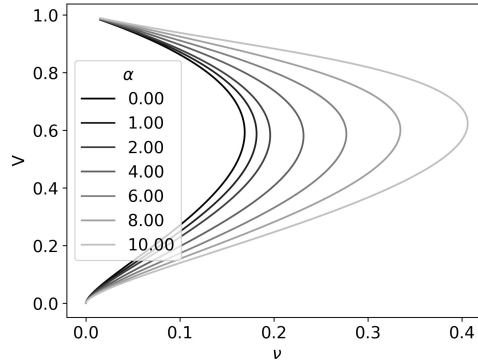


Figure 8: Locus of the velocities, V , as a function of the heat losses, ν , for different Lewis number parameters, α . Global heat losses.

For the case in which the heat losses outside the flamelets are disregarded, Eqs. (38)-(46) provide the required profiles. Figures 11 to 16 depict results for various heat losses at $\alpha = 1$. Figures 11, 13 and 15 show the profiles for the upper branch, whilst Figures 12, 14 and 16 the profiles for the lower branch.

In Figures 11-12 one observes a steep slope of the curves on the left compared to a relatively slow decay on the right.

A much more realistic temperature profile arises considering higher orders of the $1/\beta$ -expansions, Figures 13-14.

The profiles for global heat losses are shown in Figures 17 to 22.

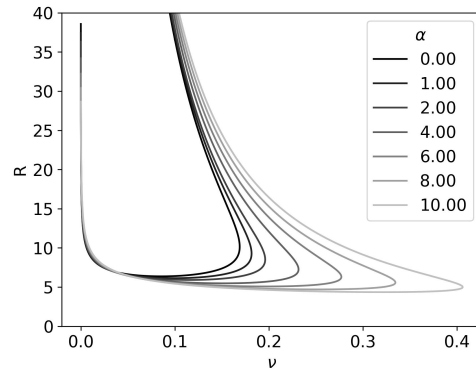


Figure 9: Locus of the flamelet radii, R , as a function of the heat losses, ν , for different Lewis number parameters, α . Global heat losses.

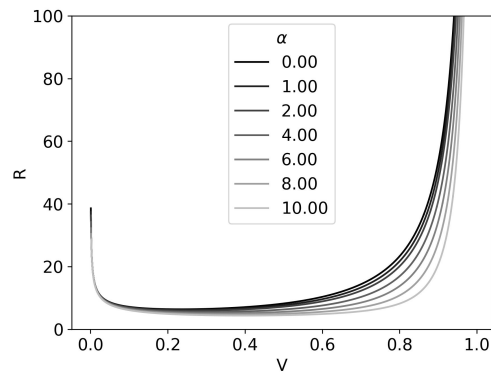


Figure 10: Locus of the flamelet radii, R , as a function of the velocities, V , for different Lewis number parameters, α . Global heat losses.

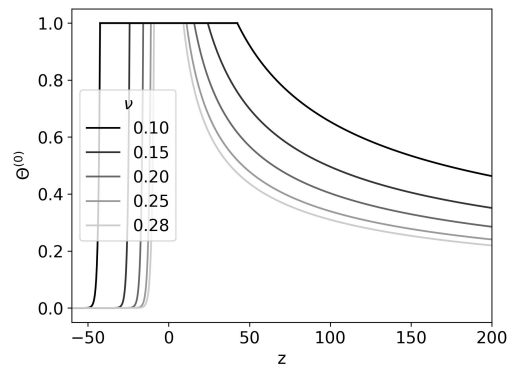


Figure 11: Profiles of $\Theta^{(0)}$ for $\alpha = 1$ and different values of ν for inner losses. Upper branch.

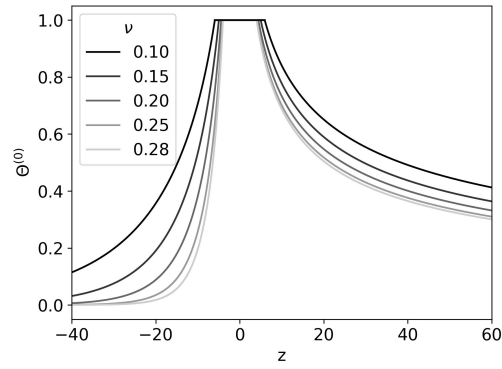


Figure 12: Profiles of $\Theta^{(0)}$ for $\alpha = 1$ and different values of ν for inner losses. Lower branch.

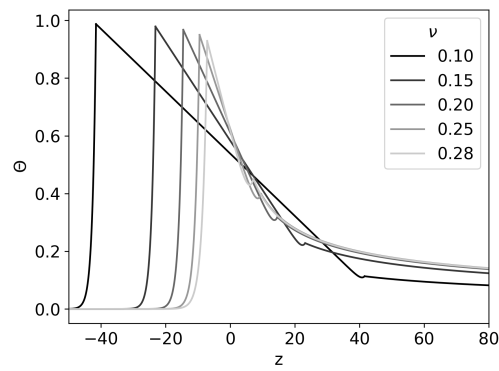


Figure 13: Profiles of Θ for $\alpha = 1$, $\beta = 10$ and different values of ν for inner losses. Upper branch.

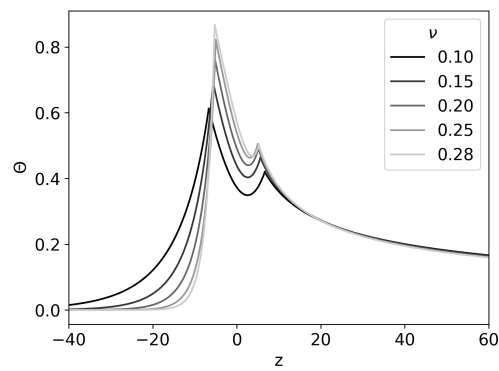


Figure 14: Profiles of Θ for $\alpha = 1$, $\beta = 10$ and different values of ν for inner losses. Lower branch.

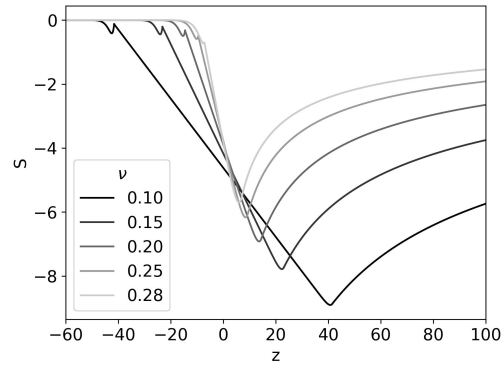


Figure 15: Profiles of S for $\alpha = 1$ and different values of ν for inner losses. Upper branch.

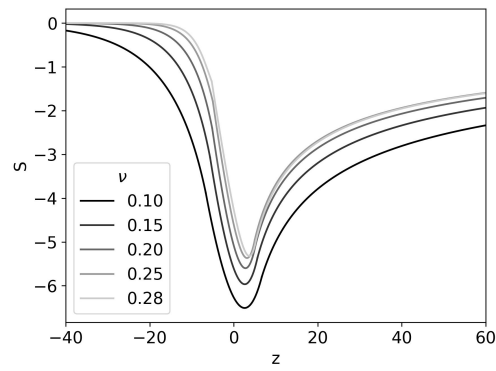


Figure 16: Profiles of S for $\alpha = 1$ and different values of ν for inner losses. Lower branch.

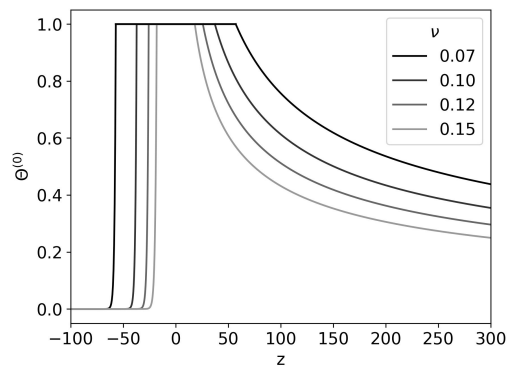


Figure 17: Profiles of $\Theta^{(0)}$ for $\alpha = 1$ and different values of ν for global losses. Upper branch.

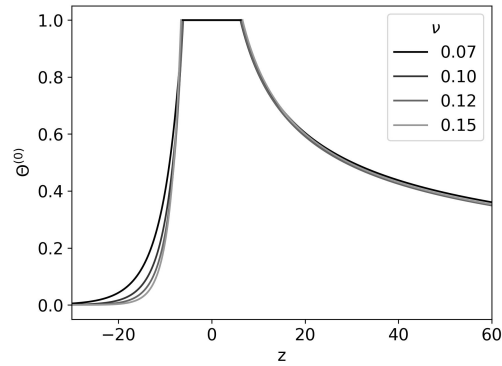


Figure 18: Profiles of $\Theta^{(0)}$ for $\alpha = 1$ and different values of ν for global losses. Lower branch.

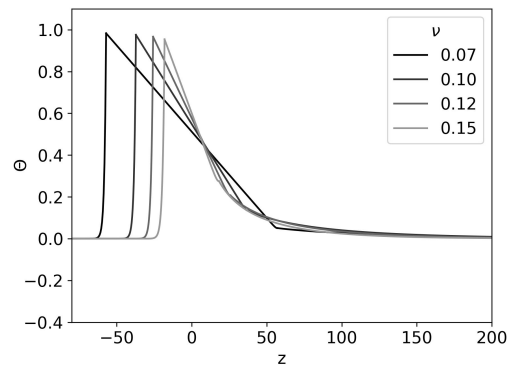


Figure 19: Profiles of Θ for $\alpha = 1$, $\beta = 10$ and different values of ν for global losses. Upper branch. Uniform approximation.

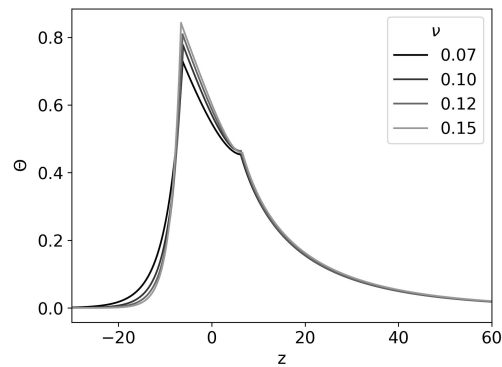


Figure 20: Profiles of Θ for $\alpha = 1$, $\beta = 10$ and different values of ν for global losses. Lower branch. Uniform approximation.

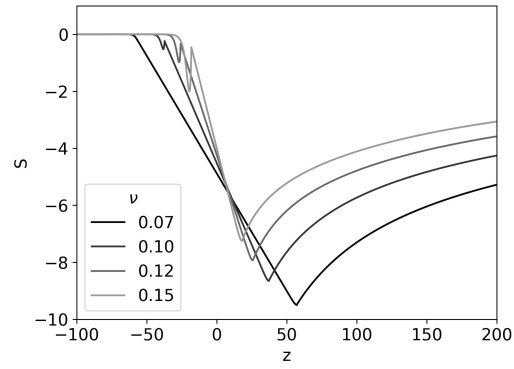


Figure 21: Profiles of S for $\alpha = 1$ and different values of ν for global losses. Upper branch. Uniform approximation.

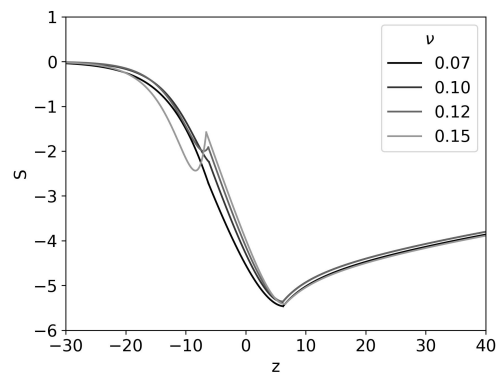


Figure 22: Profiles of S for $\alpha = 1$ and different values of ν for global losses. Lower branch. Uniform approximation.

4 Conclusions

This article constitutes a theoretical contribution to the studies of the flame front disintegration in Hele-Shaw cells [14, 15, 16, 30]. The adopted approach is conceptually linked to the theory of Zeldovich et al. [1] of flame-balls stabilized by heat losses. The phenomenon is explored employing a simplified 1D model. As a result we were able to calculate the radius-velocity-Lewis number-heat losses locus allowing for 2D self-drifting flame-balls.

Two branches of small-large radius, and low-high velocity are revealed for the same level of heat losses –aka gap between Hele-Shaw plates.

The 2D flame-balls have a fundamental characteristic which distinguishes them from their 3D counterparts. Specifically, one of the principal outcomes of [18] is that a 3D self-drifting flame-ball emerges as a bifurcation from a steady spherical structure. This bifurcation was later confirmed by Minaev et al. [19, 20, 21] through a rigorous mathematical analysis of a 3D model.

The lack of a steady solution and a bifurcation is one of the basic differences between the 3D studies and the results of our analysis dealing with 2D flamelets.

The present work is devoted to estimates of the propagation velocity of an individual flame ball in a flat channel. It would be interesting to extend the analysis over the collective propagation of a group of flame balls as appears in Figs. 1-3, and where the flamelets compete for the common fuel and mutual heating of one another. A mean-field type of approach as that developed by D'Angelo and Joulin [31] or Willimas and Grcar [32] seems particularly promising.

In our understanding of the phenomenon, flame-balls emerge in gaseous premixtures as an extreme case of diffusive-thermal instability where invariably $Le < 1$. A similar pattern is observed in smoldering burning of thin solid sheets with and without flows [33, 35, 34, 36, 37, 38, 39, 40]. It would be interesting to extend the 1D approach of this paper also to the above gas-solid configurations.

Acknowledgements

This research was supported in part by the US-Israel Binational Science Foundation (Grant 2020-005).

References

- [1] I. Zeldovich, G. Barenblatt, V. Librovich, and G. Makhviladze. *Mathematical Theory of Combustion and Explosions*. Consultants Bureau, New York, NY, 1985.
- [2] Ya. Zeldovich. *Selected Works of Yakov Borisovich Zeldovich, Volume I: Chemical Physics and Hydrodynamics*. Princeton University Press, 1992.
- [3] P. Ronney. Near-limit flame structures at low lewis number. *Combust. Flame*, 82:1–14, 1990.
- [4] P. D Ronney, M.-S. Wu, H. Pearlman, and K. Weiland. Experimental study of flame balls in space: Preliminary results from sts-83. *AIAA J.*, 36:1361–1368, 1998.
- [5] J. Buckmaster, G. Joulin, and P. Ronney. The structure and stability of nonadiabatic flame balls. *Combust. Flame*, 79:381–392, 1990.
- [6] J. Buckmaster, G. Joulin, and P. Ronney. The structure and stability of nonadiabatic flame balls: Ii. effects of far-field losses. *Combust. Flame*, 84:411–422, 1991.
- [7] J. Buckmaster and G. Joulin. Influence of boundary-induced losses on the structure and dynamics of flame-balls. *Combust. Sci. Technol.*, 89:57–69, 1993.
- [8] J. Buckmaster and G. Joulin. Flame balls stabilized by suspension in fluid with a steady linear ambient velocity distribution. *J. Fluid Mech.*, 227:407–427, 1991.
- [9] J. Buckmaster, M Smooke, and V Giovangigli. Analytical and numerical modeling of flame-balls in hydrogen-air mixtures. *Combust. Flame*, 94:113–124, 1993.
- [10] H. Bockhorn, J. Fröhlich, and K. Schneider. An adaptive two-dimensional wavelet-vaguelette algorithm for the computation of flame balls. *Combust. Theor. Model.*, 3:177, 1999.
- [11] W. Gerlinger, K. Schneider, and H. Bockhorn. Numerical simulation of three-dimensional instabilities of spherical flame structures. *Proc. Combust. Inst.*, 28:793–799, 2000.
- [12] W. Gerlinger, K. Schneider, J. Fröhlich, and H. Bockhorn. Numerical simulations on the stability of spherical flame structures. *Combust. Flame*, 132:247–271, 2003.

- [13] J. Grcar. A new type of steady and stable, laminar, premixed flame in ultra-lean, hydrogen–air combustion. *Proc. Combust. Inst.*, 32:1011–1018, 2009.
- [14] F. Veiga-López, M. Kuznetsov, D. Martínez-Ruiz, E. Fernández-Tarrazo, J. Grune, and M. Sánchez-Sanz. Unexpected propagation of ultra-lean hydrogen flames in narrow gaps. *Phys. Rev. Lett.*, 124:174501, 2020.
- [15] J.Y. Escanciano, M. Kuznetsov, and F. Veiga-López. Characterization of unconventional hydrogen flame propagation in narrow gaps. *Phys. Rev. E*, 103:033101, 2021.
- [16] D. Martínez-Ruiz, F. Veiga-López, D. Fernández-Galisteo, V. Kurdyumov, and M. Sánchez-Sanz. The role of conductive heat losses on the formation of isolated flame cells in Hele-Shaw chambers. *Combust. Flame*, 209:187–199, 2019.
- [17] L. Kagan and G. Sivashinsky. Self-fragmentation of nonadiabatic cellular flames. *Combust. Flame*, 108:220–226, 1997.
- [18] I Brailovsky and GI Sivashinsky. On stationary and travelling flame balls. *Combust. Flame*, 110:524–529, 1997.
- [19] S. Minaev, L. Kagan, G. Joulin, and G. Sivashinsky. On self-drifting flame balls. *Combust. Theor. Model.*, 5:609–622, 2001.
- [20] S. Minaev, L. Kagan, and G. Sivashinsky. Self-propagation of a diffuse combustion spot in premixed gases. *Combust. Explo. Shock+*, 38:9–18, 2002.
- [21] L. Kagan, S. Minaev, and G. Sivashinsky. On self-drifting flame balls. *Math. Comput. Simulat.*, 65:511–520, 2004.
- [22] J. Yanez, M. Kuznetsov, and F. Veiga-López. On the velocity, size, and temperature of gaseous dendritic flames. *Phys. Fluids*, 34:113601, 2022.
- [23] B. Matkowsky and G. Sivashinsky. An asymptotic derivation of two models in flame theory associated with the constant density approximation. *SIAM J. App. Math.*, 37:686–699, 1979.
- [24] H. Lamb. *Hydrodynamics*. Cambridge University Press, 1924.
- [25] S. Tomotika and T. Aoi. The steady flow of viscous fluid past a sphere and circular cylinder at small Reynolds numbers. *Q. J. Mech. Appl. Math.*, 3:141–161, 1950.
- [26] R. Seydel. *Practical bifurcation and stability analysis*, volume 5. Springer Science & Business Media, 2009.
- [27] A. Meurer, C. Smith, M. Paprocki, O. Čertík, S. Kirpichev, M. Rocklin, A. Kumar, S. Ivanov, J. Moore, S. Singh, T. Rathnayake, S. Vig, B. Granger, R. Muller, F. Bonazzi, H. Gupta, S. Vats, F. Johansson, F. Pedregosa, M. Curry, A. Terrel, Š. Roučka, A. Saboo, I. Fernando, S. Kulal, Robert Cimrman, and Anthony Scopatz. Sympy: symbolic computing in python. *PeerJ Computer Science*, 3:e103, January 2017.
- [28] M. Kuznetsov, J. Yanez, and F. Veiga-López. Near limit flame propagation in a thin layer geometry at low Peclet numbers. In *Proc. 18th Int. Conference on Flow Dynamics (ICFD 2021)*, number 8 in OS1, pages 688–692, October 2022.
- [29] G. Sivashinsky and B. Matkowsky. On the stability of nonadiabatic flames. *SIAM Journal on Applied Mathematics*, 40(2):255–260, 1981.
- [30] A. Domínguez-González, D. Martínez-Ruiz, and M. Sánchez-Sanz. Stable circular and double-cell lean hydrogen-air premixed flames in quasi two-dimensional channels. *Proc. Combust. Inst.*, 39(1):1731–1741, 2022.
- [31] Y. D’Angelo and G. Joulin. Collective effects and dynamics of non-adiabatic flame balls. *Combustion Theory and Modelling*, 5(1):1, 2001.
- [32] F. Williams and Joseph F Grcar. A hypothetical burning-velocity formula for very lean hydrogen–air mixtures. *Proceedings of the Combustion Institute*, 32(1):1351–1357, 2009.
- [33] Y. Zhang, P. Ronney, E. Roegner, and J. Greenberg. Lewis number effects on flame spreading over thin solid fuels. *Combust. Flame*, 90:71–83, 1992.
- [34] O. Zik and E. Moses. Fingering instability in combustion: an extended view. *Phys. Rev. E*, 60:518, 1999.
- [35] O. Zik, Z. Olami, and Elisha Moses. Fingering instability in combustion. *Phys. Rev. Lett.*, 81:3868, 1998.
- [36] T. Matsuoka, K. Nakashima, Y. Nakamura, and S. Noda. Appearance of flamelets spreading over thermally thick fuel. *Proc. Combust. Inst.*, 36:3019–3026, 2017.
- [37] F. Zhu, Z. Lu, S. Wang, and Y. Yin. Microgravity diffusion flame spread over a thick solid in step-changed low-velocity opposed flows. *Combust. Flame*, 205:55–67, 2019.
- [38] J. Malchi, R. Yetter, S. Son, and G. Risha. Nano-aluminum flame spread with fingering combustion instabilities. *Proc. Combust. Inst.*, 31(2):2617–2624, 2007.

-
- [39] S. Olson, H. Baum, and T. Kashiwagi. Finger-like smoldering over thin cellulosic sheets in microgravity. In *Symp. (Int.) Combust.*, volume 27, pages 2525–2533. Elsevier, 1998.
- [40] Y. Uchida, K. Kuwana, and G. Kushida. Experimental validation of lewis number and convection effects on the smoldering combustion of a thin solid in a narrow space. *Combustion and Flame*, 162(5):1957–1963, 2015.